Radiological Physics and Technology (2019) 12:374–381
https://doi.org/10.1007/s12194-019-00532-8

A comparative study of radiation doses between phantom and patients via CT angiography of the intra-/extra-cranial, pulmonary, and abdominal/pelvic arteries

M. K. A. Karim[1] · A. Sabarudin[2] · N. A. Muhammad[1] · K. H. Ng[3]

Received: 18 February 2019 / Revised: 9 August 2019 / Accepted: 10 August 2019 / Published online: 29 August 2019

Abstract
This study aimed to evaluate effective dose and size-specific dose estimate (SSDE) of computed tomography angiography (CTA) examination using an anthropomorphic phantom. We included three CTA examination protocols to evaluate the intra- and extra-cranial arteries, pulmonary artery (CTPA), and abdominal vessels. Patient SSDEs were measured retrospectively to estimate patient dose, relative to the bodyweight of the patient and volume CT dose index ($CTDI_{vol}$). Our findings revealed that the highest dose was absorbed by the left lobe of the thyroid gland during intra-/extra-cranial CTA and CTPA, that is, 14.11 ± 0.24 mGy and 16.20 ± 3.95 mGy, respectively. However, the highest absorbed dose in abdominal/pelvic CTA was the gonads (8.98 ± 0.30 mGy), while other radiosensitive organs in intra- and extra-cranial CTA, CTPA, and abdominal/pelvic CTA did not demonstrate significant differences between organs/structures with p value 0.88, 0.11, and 0.54, respectively. The estimated effective dose in intra-/extra-cranial CTA was lower in patients (0.80 ± 0.60 mSv) than in the phantom (0.83 mSv), but it was the opposite for CTPA, with the effective dose being higher in patients (7.54 ± 3.09 mSv) than in the phantom (6.68 mSv). Similar to the effective dose, only CTPA SSDEs were significantly higher in men than in women (19.74 ± 4.79 mGy versus 7.9 mGy). Effective dose and SSDE are clinically relevant parameters that can help estimate a more accurate patient dose based on a patient's size.

Keywords CT angiography · Effective dose · Dose-length product · Absorbed dose · Size-specific dose estimate

1 Introduction

Catheter-based angiography is widely used to accurately visualize the anatomic details of blood vessels for diagnosis and therapy, but the risk of developing an infection from interventional procedure is still an inevitable problem. Currently, angiography can be performed using a CT scan, that incorporates an interventional technique with a slip-ring gantry technology and multi-row detector arrays, and is responsible for significantly improving angiography in the field of clinical imaging. CT angiography (CTA) can provide high contrast images of the vascular anatomy, including multiple planes with specialized volumetric data. This improves the specificity and sensitivity of diagnosing cardiovascular diseases [1]. Furthermore, CTA has made it possible to visualize vascular structures far beyond the contrast column, demonstrating numerous vascular pathologies, including atherosclerosis, thrombus, inflammatory changes, and extravascular hemorrhage [2, 3].

Although differentiating the vasculature from bony structures is of paramount importance, it is technically difficult to perform. In this regard, CTA offers numerous potential advantages over conventional angiography with C-arm fluoroscopy. Previous studies on image quality have meticulously reported that CTA can produce images with relatively higher contrast without significant artefacts, particularly in blood-flow imaging [4–6]. Despite its beneficial features, radiation exposure from CTA remains the greatest concern among radiology personnel [7]. Furthermore, because of its

✉ M. K. A. Karim
khalis.karim@gmail.com

[1] Department of Physics, Faculty of Science, Universiti Putra Malaysia, 43400 Serdang, Selangor, Malaysia

[2] Programme of Diagnostic Imaging and Radiotherapy, Faculty of Health Sciences, Universiti Kebangsaan Malaysia, 56000 Kuala Lumpur, Malaysia

[3] Department of Biomedical Imaging, Faculty of Medicine, University of Malaya, 50603 Kuala Lumpur, Malaysia

complex acquisition parameters and long scanning time, it is one of the highest sources of radiation dose exposure among all CT techniques, apart from other interventional radiology techniques.

Exposure to high doses of radiation can produce detrimental effects on the radiosensitive organs, such as the eye lens, pituitary gland, thyroid gland, breast, and skin [8, 9]. Hence, it is essential for personnel to monitor the radiation dose that a patient is exposed to during CTA. Globally, different authorities have emphasized the importance of radiation protection, mandated the implementation of low-dose protocols, and implemented safety measures based on studies [10, 11]. Therefore, the aim of this study is to determine the effective dose and size-specific dose estimates (SSDE) in common CTA examinations (extra- and intra-cranial, pulmonary, and abdominal aorta) as reflected by the anthropomorphic phantom.

2 Materials and methods

The CTA procedure was performed according to standard protocols, as it was a routine clinical practice in our institution. The research protocols were approved by the institution's research ethical committee with ethical number UKMPPI/111/8/JEP-2018-012. The study was divided into two parts, where the first part was an experimental study that performed on an Alderson-Rando anthropomorphic phantom (Alderson Research Laboratories, Long Island, New York, USA), as shown in Fig. 1. The phantom was configured as an adult male, 1.75 m in height, and weighing 73.5 kg. This phantom comprised 34 slabs containing tissue equivalent materials each having a thickness of 2.5 cm with a small hole to place the thermoluminescence dosimeters (TLD-100) chips (Thermo Fisher Scientific, Waltham, Massachusetts, USA) [12].

In the second part, we retrieved scanning data of 70 patients who were subjected to intra- and extra-cranial ($n=26$), pulmonary ($n=8$), and abdominal/pelvic ($n=36$) CTA between January and December 2016 at the Radiology Department of a teaching hospital in Kuala Lumpur. Subject's demographics (age, sex, and race) and acquisition parameters (tube current, longitudinal scan range, tube voltage, and pitch) were recorded in a standardized form.

2.1 Radiation dose measurements

2.1.1 Organ-absorbed dose

TLD-100 chips containing lithium fluoride doped with magnesium, copper, and phosphorus (LiF: Mg, Cu, P) were used to measure the organ-absorbed dose. The TLDs were inserted into the special holes of the phantom in positions

Fig. 1 Alderson-Rando phantom with multiple slabs for radiation dose monitoring. The hole in each slab is designed for TLD chip placement for organ dose measurement

representing the dedicated organs. A total of 18 TLD chips were used for each of the three CTA protocols in this study. The TLD chips for intra- and extra-cranial CTA were placed on slab no. 3, which represented the eye lenses; those for CT pulmonary angiography (CTPA) were inserted into slab nos. 8 and 15, which represented the thyroid and breasts; and those for abdominal/pelvic CTA were placed in the gonadal region (slab no. 34). The chips were also placed in the seventh thoracic vertebra (T7) (slab no. 17) and iliac crest region (slab no. 28) to represent the skin in CTPA and abdominal/pelvic CTA.

Three TLD chips were used as a control for background measurement. Each study was repeated three times, and the value of the TLD reading for each organ was averaged from the organ-absorbed doses. The TLD chips were sent for a readout process 24 h after irradiation using the Harshaw TLD Reader Model 3500 (Thermo Electron Corporation, Solon, Ohio, USA). This process ensured that any residual luminescence signals from the short half-life peak did not significantly affect the actual signal during the process. The TLDs' measurement in the Rando phantom was considered versatile, as it determines organ dose in-direct contact [13, 14]. To obtain the actual value of measurement, the TLD readings were converted to organ-absorbed dose in the phantom using the following equation:

$$D_t = \text{reading TL} \times \text{CF}, \quad (1)$$

where D_t is an organ-absorbed dose, reading TL is the measurement obtained from the TLD reader, and CF is an

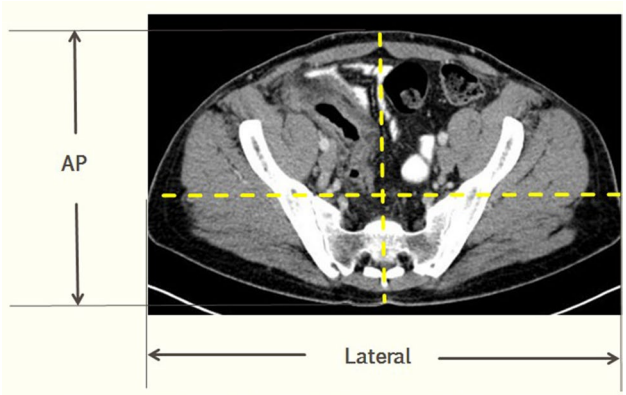

Fig. 2 Two measurements required on patient's image represented by *x*-axis (AP) and *y*-axis (lateral) for obtaining SSDE values

individual conversion factor obtained from the calibration study. The final product of absorbed dose must include tissue-energy dependent measurement, taking the inhomogeneity of tissue within the selected region into consideration. Therefore, the biological tissue dose at a certain depth, in particular for the breasts and thyroid, can be calculated based on the cavity approach using the equation below:

$$D_{f,z} = D_t\left[\left(\frac{\bar{\mu}_{en}}{\rho}\right)\right]. \quad (2)$$

Here, $D_{f,z}$ is the organ-absorbed dose at a certain depth, and $\frac{\bar{\mu}_{en}}{\rho}$ is the ratio of the mass-energy absorption coefficients for the water to air obtained from the study by Ma et al. [15].

2.1.2 SSDE calculation

The concept of SSDE was introduced by the Report of American Association of Physics in Medicine (AAPM) Task group 204, which allows the estimation of the CT radiation dose based on the $CTDI_{vol}$ value and patient body diameter. SSDE could be calculated either before or after CT examinations using the $CTDI_{vol}$ value provided by the scanner. The SSDE of the patients was determined retrospectively using the following equation:

$$SSDE = f_{size}CTDI_{vol}, \quad (3)$$

where f_{size} is the conversion factor obtained from the AAPM 204 report based on CTDI phantom, which has a diameter of 16 cm or 32 cm; $CTDI_{vol}$, in mGy, was obtained from the operation console. The conversion factor, f_{size}, was obtained from the anteroposterior (representing width) and lateral (representing depth) dimensions of the widest slices of the regions of interest, as illustrated in Fig. 2. The effective diameter was measured based on the following equation provided by AAPM:

$$\text{Effective diameter} = \sqrt{AP \times \text{lateral}}. \quad (4)$$

2.1.3 Effective dose measurement

In this study, we derived the effective dose from the product of dose-length product (DLP) and a conversion coefficient *(k)* based on the anatomic region. The *k* value for the head and neck was 2.2 µSv/mGy cm, that for the chest was 20.4 µSv/mGy cm, and that for the abdomen/pelvis was 17.1 µSv/mGy cm [16, 17]. These coefficients were determined based on the data of organ-weighting factors by considering tissue dose coefficients using Monte Carlo (MC) calculations and the measurement specified by the International Commission on Radiological Protection (ICRP). This measurement technique has been shown to be practically robust and is widely used to estimate the effective dose for CT examination.

2.1.4 CTA protocols

All scans were performed on the 64-slice Siemens Somatom Sensation 64 scanner (Siemens Medical Solutions AG, Munich, Germany) using the CARE Dose4D low radiation dose protocol. In general, CTA examination involved a series of scanning procedures inclusive of topography or scanography, contrast enhancement using automated bolus triggering or test bolus methods, and actual scan acquisition. All actual scanning acquisitions were constructed on a similar scout image to visualize topography with an identical coverage volume, to maintain the uniformity of the study pattern. All the acquisition parameters are presented in Table 1.

First, we performed intra- and extra-cranial CTA scanography to function as a reference, which included anteroposterior (AP) and lateral (LAT) images of the head and neck that encompassed the skull vertex to C7/T1 of the vertebra, including the frontal and occipital bones. The scan was followed by volumetric scanning of the head and neck regions with a scanning field of view (SFOV) that included the entire brain and soft tissues of the neck, such that the cerebral arteries, the circle of Willis, and internal and external carotid arteries were within the field of view (FOV). A minimum of 70 mL iopamidol (350 mgI/mL) contrast solution (Bracco Imaging, Milano, Italy) was injected intravenously at a flow rate of 4.5–5.0 mL/s, followed by 10 mL saline flush at 4.5 mL/s. Automated bolus triggering technique was used to track the bolus in the region of interest, specifically at the aortic arch, with a baseline threshold of 60 HU.

Table 1 Intra-/extra-cranial, pulmonary, and abdominal/pelvic CT angiography protocols for patients and the Alderson-Rando phantom

Parameters	Intra-/extra-cranial	Pulmonary	Abdomen/pelvis
Collimation (mm)	64×0.6	64×0.6	64×0.6
Scanning mode	Helical	Helical	Helical
Slice thickness (mm)	3.0	3.0	5.0
Pitch	0.9	0.9	0.9
Rotation time (s)	0.37	0.5	0.5
Tube voltage (kV)	140	140	140
Reference noise (in mAs)	250	160	200
Scan time (s)	5.90	7.58	9.89
Scan length (mm)	180.0	389.0	410.0
Orientation	Craniocaudal	Craniocaudal	Caudocranial

In CTPA, the scout image was obtained from the chin to diaphragm, including the heart. The actual scan was followed by a helical scan, in which SFOV included the area from C4 to L2/L3 of the intervertebral disks with a fine slice thickness of 0.625 mm. A minimum of 60 mL Iopamiro (350 mgI/ml) contrast agent was injected intravenously at a flow rate of 4.5–5.0 mL/s, followed by 10 mL saline flush at 4.5 mL/s. To achieve a better image enhancement, a test bolus was used in this examination rather than automated bolus triggering. The use of bolus triggering in CTPA was not recommended, because the contrast medium would be rapidly flushed away from the pulmonary arteries. The optimal scan delay time for the actual study was presumed to be the time required for the image to show maximum enhancement at the pulmonary trunk from the time of the test bolus injection.

In abdominal/pelvic CTA, the scanogram covered the dome of the diaphragm to the pubic symphysis. Data acquisition included the abdominal and pelvic regions in entirety to obtain information on abdominal aorta and iliac arteries. A minimum of 80 mL iopamiro (350 mgI/mL) contrast agent was administered intravenously at a flow rate of 4.5–5.0 mL/s, followed by 10 mL saline flush at 4.5 mL/s. The automated bolus-triggering technique was used to track the bolus in the regions of interest, specifically the abdominal aorta at the level of the adrenal gland, with a baseline threshold of 90 HU.

2.2 Statistical analysis

The data were analyzed using the Statistical Package for the Social Sciences Version 21 (IBM SPSS, Armonk, New York, USA). One-way analysis of variance (ANOVA) and post hoc test were used to compare absorbed doses in critical organs in all three CTA examinations ($p < 0.05$). The independent t test was applied to compare the means of estimated effective dose and SSDE between sexes ($p < 0.05$), and the one sample t test was used to compare the means of the estimated effective dose of patients ($p < 0.05$).

Table 2 Absorbed doses of radiosensitive organs in intra-/extra-cranial, pulmonary, and abdominal/pelvic CT angiography protocols on the Alderson-Rando phantom

Radiosensitive organs/protocols	CTA intra-/extra-cranial (mGy)	CTPA (mGy)	CTA abdomen/pelvis (mGy)
Right eye lens	10.11 ± 0.30	NM	NM
Left eye lens	10.38 ± 0.56	NM	NM
Pituitary gland	8.21 ± 0.04	NM	NM
Right thyroid	13.81 ± 0.42	16.76 ± 3.21	NM
Left thyroid	14.91 ± 0.24	17.12 ± 3.95	NM
Right breast	NM	12.27 ± 0.24	NM
Left breast	NM	12.95 ± 0.26	NM
Skin	NM	12.95 ± 0.63	8.59 ± 0.40
Gonads	NM	NM	8.98 ± 0.30

NM not measured

3 Results

The absorbed doses of radiation for different organs/structures corresponding to different CTA examinations on the phantom are presented in Table 2. The highest dose was received by the left lobe of the thyroid gland in intra-/extra-cranial CTA and CTPA that was 14.11 ± 0.24 mGy and 16.20 ± 3.95 mGy, respectively. However, the highest absorbed dose in abdominal/pelvic CTA was in the gonads (8.98 ± 0.30 mGy). The absorbed doses of the remaining radiosensitive organs in intra-/extra-cranial CTA, CTPA, and abdominal/pelvic CTA were not significantly different from organs/structures with p values of 0.88, 0.11, and 0.54, respectively.

The mean effective dose value and SSDE between the patients and phantom are compared in Figs. 3 and 4. The estimated effective dose in intra-/extra-cranial CTA was

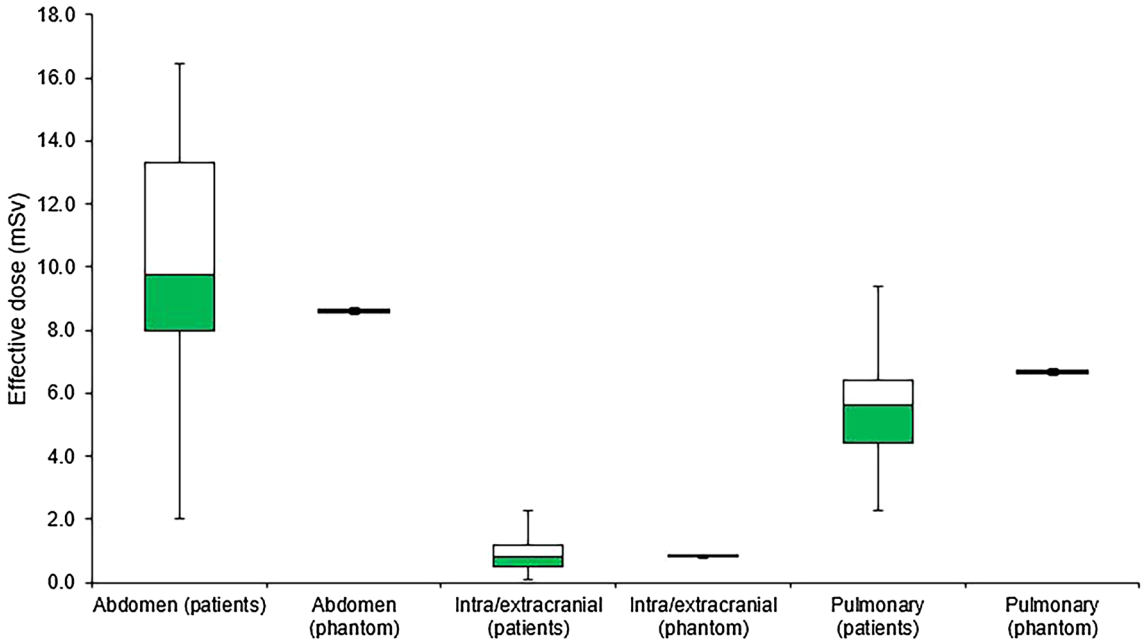

Fig. 3 Effective dose comparison between patients' data at the Department of Radiology and Alderson-Rando phantom in the examination of abdomen/pelvis, intra-/extra-cranial, and pulmonary CT angiography, showing that intra-/extra-cranial CTA procedures produce the lowest effective dose compared to the other CTA examinations. The boxes indicate the first to the third quartiles; each midline indicates the median (second quartile), and the whiskers represent the maximum and minimum values of effective dose

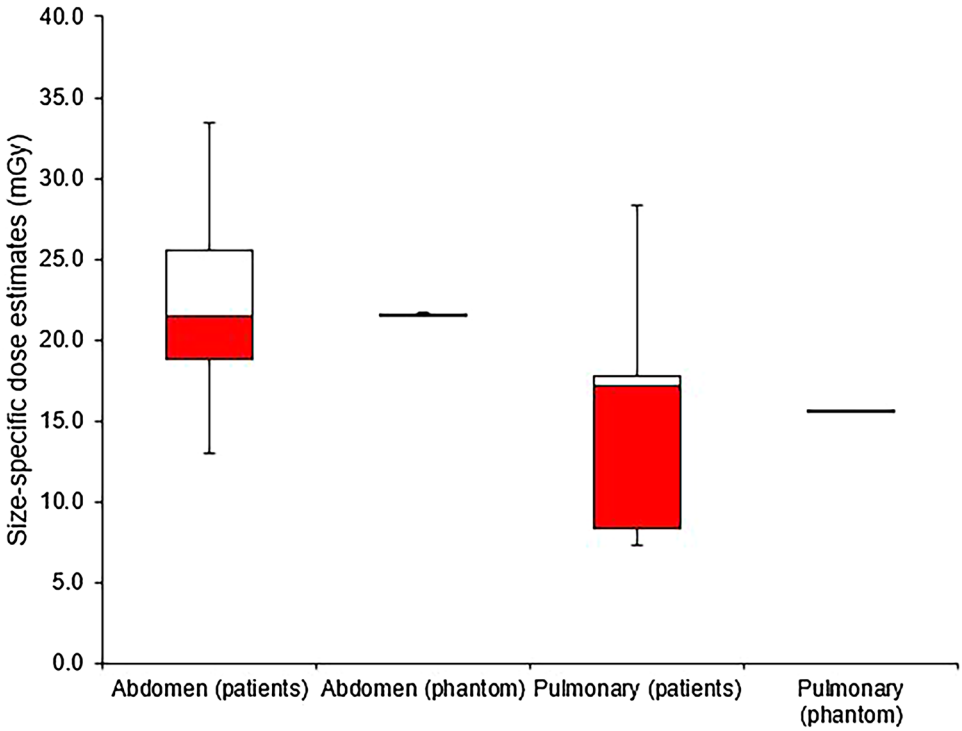

Fig. 4 Size-specific dose estimation (SSDE) between patients' data at the Department of Radiology and Alderson-Rando phantom in the examination of abdomen/pelvis, intra-/extra-cranial, and pulmonary CT angiography. It shows that abdomen/pelvis CTA procedure produces the highest SSDE value compared to the other CTA examinations. The boxes indicate the first to the third quartiles; each midline indicates the median (second quartile), and the whiskers represent the maximum and minimum values of SSDE

lower in patients (0.80 ± 0.60 mSv) than in the phantom (0.83 mSv), contrary to the CTPA, in which the effective dose was higher in patients (7.54 ± 3.09 mSv) than in the phantom (6.68 mSv). The estimated effective dose of the abdominal/pelvic CTA was significantly higher in patients (11.88 ± 3.85 mSv) than in the phantom (8.66 mSv) ($p < 0.05$). Dose comparison revealed a significant difference in the CTPA, where male patients received a higher

Table 3 Mean estimated effective dose (ED) and SSDE of intra-/extra-cranial, CTPA, and abdominal/pelvic CTA

Radiation dose	CTA intra-/extra-cranial	CTPA	CTA Abdomen/pelvis
Male			
ED (in mSv)	0.85 ± 0.41	9.24 ± 2.36	12.12 ± 1.34
SSDE (in mGy)	n/a	19.74 ± 4.79	22.65 ± 4.12
Female			
ED (in mSv)	0.74 ± 0.32	4.71 ± 1.74	11.10 ± 2.86
SSDE (in mGy)	n/a	7.88 ± 0.55	21.15 ± 3.32
Phantom			
ED (in mSv)	0.83	6.68	8.66
SSDE (in mGy)	7.80	15.70	21.90

n/a not applicable

effective dose than female patients (9.24 ± 2.36 mSv versus 4.71 ± 1.74 mSv) ($p < 0.05$), as shown in Table 3. The remaining CTA examinations showed that the effective doses were lower in male patients than in female patients, but were not significant.

Despite all three CTA examinations showing insignificant differences, the SSDE of patients seemed to be higher than that of the phantom in abdominal/pelvic CTA (22.49 ± 5.39 mGy versus 21.9 mGy). The mean SSDE corresponding to CTPA in the phantom study (15.7 mGy) was non-significantly higher than that in patients (15.30 ± 7.13 mGy). Similar to effective dose, only CTPA showed significantly higher SSDE in male patients than in female patients (19.74 ± 4.79 mGy versus 7.9 mGy). Furthermore, in the remaining CTA examinations, SSDE was lower in male patients than in female patients, but the differences were not statistically significant.

4 Discussion

Three conclusions can be derived from this study. First, as there were no significant differences in the effective dose and SSDE between the phantom and patients, this means that the absorbed dose in radiosensitive organs of the patients could be estimated using the technique demonstrated in this phantom study. Second, estimated effective doses and SSDE did not report significant differences between the sexes in CTA examinations, with the exception of CTPA. This suggests that variations in the male and female body might lead to discrepancies in results of the radiation dose. Finally, SSDE measurements could improve the accuracy of volume dose calculation, and it produced better results than the CT dose index volume ($CTDI_{vol}$).

Effective dose is a key parameter that could provide an insight into the relative risk of exposure to ionizing radiation. Two methods could be used to estimate that dose. The first was based on organ-equivalent dose estimates utilizing tissue-weighting coefficients. In the second method proposed by ICRP, effective dose could be calculated by multiplying the DLP with a conversion coefficient factor k, which depended on the anatomical region being scanned. In addition, AAPM also proposed another dose descriptor, namely, the SSDE to epitomize a more accurate estimation of patient doses by taking body diameter into consideration, which would enable users to optimize $CTDI_{vol}$ based on a patient's habitus [18, 19].

Our study revealed that estimated effective doses were similar to those defined in the European guidelines. Based on the "European Guideline" for CT doses, the mean effective doses for the head and neck, pulmonary, and abdominal/pelvic CTA were 1–2 mSv, 5–7 mSv, and 8–14 mSv, respectively [20]. However, the estimated effective dose for the head and neck procedure was slightly lower than that recommended by the European Guidelines for CTA procedures. This variation was due to differences in scanning parameters, such as exposure factors (kVp and mAs), pitch, and gantry rotation time.

The SSDE of male patients who underwent CTA of the head and neck and abdomen/pelvis was slightly lower than that of female patients. Contrarily, the male patients who underwent CTPA showed significantly higher SSDE than their corresponding female patients. The AAPM Report 204 had stated that SSDE was indisputably accurate compared to $CTDI_{vol}$. A $CTDI_{vol}$ value provided information about the dose during the volume scan as a scanning output, which was dependent on the scanning parameters, and patient size was not a requirement [6]. Hence, $CTDI_{vol}$ could not be used as a dose reference to represent the total dose received by a patient. To accurately measure the dose received by a patient in each CT examination, the patient's dimensions must be considered. Two orthogonal dimensions must be recorded; these are represented by LAT length, which is measured from right to left (x-axis), and AP length, measured from anterior to posterior (y-axis).

Furthermore, other complex estimations can be conducted using the sum of AP and LAT, which is the effective diameter (square root of the product of AP and LAT). In the present study, all dimensions were determined using an electronic caliper. In addition, a conversion factor for effective diameter was provided by AAPM Report 204 based on polymethyl methacrylate cylindrical reference phantoms with diameters of 16 cm and 32 cm. While a phantom with a diameter of 16 cm was designed for adult head and pediatric body scan protocol, a phantom with a diameter of 32 cm was used for body trunk examinations covering the

chest, abdomen, and pelvis [21]. $CTDI_{vol}$ and effective body diameter (AP + LAT dimensions) were required to determine SSDE.

In addition to being considered the best examination procedure for detecting pulmonary embolism, CT pulmonary angiography has other advantages—it is fast, reliable, and readily available in diagnostic centers globally. Patients are exposed to a very low doses of radiation, approximately 10 mSv per examination [22]. According to the CTPA protocol, a collimation that allowed thinner slices, which was 3.0 mm rather than 5.0 mm, could be used to provide sufficient visualization of up to 94% of sub-segmental arteries and enable the detection of micro-emboli in the pulmonary arteries [23, 24].

Among the various regions of the body, the thoracic cavity demonstrated poor radiation absorption and possibly inherent high contrast between the vascular and interstitial structures. In addition, the hollow structure allowed the required quantity of radiation to penetrate with minimum tube voltage. Furthermore, the introduction of iodinated contrast medium into this protocol improved the image quality, because the effective energy of X-ray beams would decrease while optimizing absorption to the *k*-edge of iodine [25].

The radiation-absorbed dose was estimated using a standardized phantom based on $CTDI_{vol}$ values, and did not epitomize specific patients. Similar to this study or any passive dosimeter, measuring absorbed doses using TLD chips was regarded as the gold standard in applied radiology. Nevertheless, this measurement technique was not clinically practical, as the TLD chips had several limitations: they must be placed inside the patient's body and that could be time-consuming. Therefore, several researchers had explored the potential of quantifying the radiation doses on the basis of SSDE, which was a great initiative to monitor and optimize the exposure to CT radiation [18, 26].

There were some limitations in this study. First, the iodinated contrast medium could not be introduced in the phantom. Thus, any changes in image quality associated with CTA examinations could not be evaluated and compared, because the vascular system was unenhanced. Due to the lack of extremities, the phantom did not represent a real human anatomy, which limited the present study from estimating the absorbed dose received by the upper and lower limb regions of the patients.

5 Conclusion

In this study, effective dose and SSDE were estimated from CTA examinations. Various measurement techniques could provide different results, which suggested that dose estimation should be undertaken periodically in accordance with the "As Low as Reasonably Achievable" (ALARA) principles of radiation protection. This study provides a useful information to CT technologists and medical physicists to monitor the radiation dose received by each patient, besides optimizing the CTA examinations.

Acknowledgements The authors are grateful to the staff of HUKM for their technical assistance during the data collection process. The authors also wish to acknowledge the support received from Geran IPM Universiti Putra Malaysia (project no: GP/IPM/UPM/9619800).

Compliance with ethical standards

Conflict of interest The authors declare that they have no conflict of interest.

Ethical approval The research protocols were approved by the institution's research ethical committee with ethical number UKMPPI/111/8/JEP-2018-012.

References

1. Jayakrishnan VK, White PM, Aitken D, Crane P, McMahon AD, Teasdale EM. Subtraction helical CT angiography of intra- and extracranial vessels: technical considerations and preliminary experience. AJNR Am J Neuroradiol. 2003;24:451–5.
2. Schueller-Weidekamm C, Schaefer-Prokop CM, Weber M, Herold CJ, Prokop M. CT angiography of pulmonary arteries to detect pulmonary embolism: improvement of vascular enhancement with low kilovoltage settings. Radiology. 2006;241:899–907. https://doi.org/10.1148/radiol.2413040128.
3. Sabarudin A, Siong TW, Chin AW, Hoong NK, Karim MKA. A comparison study of radiation effective dose in ECG-gated coronary CT angiography and calcium scoring examinations performed with a dual-source CT scanner. Sci Rep. 2019;9:4374. https://doi.org/10.1038/s41598-019-40758-5.
4. Bombiński P, Warchoł S, Brzewski M, Biejat A, Dudek-Warchoł T, Krzemień G, et al. Lower-dose CT urography (CTU) with iterative reconstruction technique in children—initial experience and examination protocol. Pol J Radiol. 2014;79:137–44. https://doi.org/10.12659/PJR.890729.
5. Bischoff B, Hein F, Meyer T, Hadamitzky M, Martinoff S, Schömig A, et al. Impact of a reduced tube voltage on CT angiography and radiation dose: results of the PROTECTION I study. JACC Cardiovasc Imaging. 2009;2:940–6. https://doi.org/10.1016/j.jcmg.2009.02.015.
6. Boone JM, Brink JA, Edyvean S, Huda W, Leitz W, McCollough CH, et al. Radiation dose and image-quality assessment in computed tomography. J ICRU. 2012;12:9–149. https://doi.org/10.1093/jicru/ndt006.
7. Karim MKA, Hashim S, Bradley DA, Bahruddin NA, Ang WC, Salehhon N. Assessment of knowledge and awareness among radiology personnel regarding current computed tomography technology and radiation dose. J Phys Conf Ser. 2016;694:012031. https://doi.org/10.1088/1742-6596/694/1/012031.
8. Karim MKA, Hashim S, Sabarudin A, Bradley DA, Bahruddin NA. Evaluating organ dose and radiation risk of routine CT examinations in Johor Malaysia. Sains Malays. 2016;45:567–73.

9. Brenner DJ. Minimising medically unwarranted computed tomography scans. Ann ICRP. 2012;41:161–9. https://doi.org/10.1016/j.icrp.2012.06.004.
10. Rehani MM, Ciraj-Bjelac O, Al-Naemi HM, Al-Suwaidi JS, El-Nachef L, Khosravi HR, et al. Radiation protection of patients in diagnostic and interventional radiology in Asian countries: impact of an IAEA project. Eur J Radiol. 2012;81:e982–9. https://doi.org/10.1016/j.ejrad.2012.06.019.
11. Kalender WA, Buchenau S, Deak P, Kellermeier M, Langner O, van Straten M, et al. Technical approaches to the optimisation of CT. Phys Med. 2008;24:71–9. https://doi.org/10.1016/j.ejmp.2008.01.012.
12. Hashim S, Karim MKA, Bakar KA, Sabarudin A, Chin AW, Saripan MI, et al. Evaluation of organ doses and specific k effective dose of 64-slice CT thorax examination using an adult anthropomorphic phantom. Radiat Phys Chem. 2016;126:14–20. https://doi.org/10.1016/j.radphyschem.2016.05.004.
13. Musa Y, Hashim S, Khalis Abdul Karim M. Direct and indirect entrance surface dose measurement in X-ray diagnostics using nanoDot OSL dosimeters. J Phys Conf Ser. 2019;1248:012014. https://doi.org/10.1088/1742-6596/1248/1/012014.
14. Karim MKA, Rahim NA, Matsubara K, Hashim S, Mhareb MHA, Musa Y. The effectiveness of bismuth breast shielding with protocol optimization in CT Thorax examination. J Xray Sci Technol. 2019;27:139–47. https://doi.org/10.3233/XST-180397.
15. Ma C-M, Seuntjens JP. Mass-energy absorption coefficient and backscatter factor ratios for kilovoltage X-ray beams. Phys Med Biol. 1999;44:131–43.
16. ICRP. Compendium of Dose Coefficients based on ICRP publication 60. ICRP Publication 119. Ann ICRP. 2012;41(Suppl.).
17. Huda W, Magill D, He W. CT effective dose per dose length product using ICRP 103 weighting factors. Med Phys. 2011;38:1261. https://doi.org/10.1118/1.3544350.
18. Huda W. Computing patient specific effective doses and radiation risks in CT. Phys Med. 2012;28:333. https://doi.org/10.1016/j.ejmp.2012.06.008.
19. Pourjabbar S, Singh S, Padole A, Saini A, Blake MA, Kalra MK. Size-specific dose estimates: localizer or transverse abdominal computed tomography images? World J Radiol. 2014;6:210–7. https://doi.org/10.4329/wjr.v6.i5.210.
20. Commission E. European guidelines on quality criteria for computed tomography. EUR 16262 EN. 1997.
21. Karim MKA, Hashim S, Bradley DA, Bakar KA, Haron MR, Kayun Z. Radiation doses from computed tomography practice in Johor Bahru, Malaysia. Radiat Phys Chem. 2016;121:69–74. https://doi.org/10.1016/j.radphyschem.2015.12.020.
22. Laqmani A, Regier M, Veldhoen S, Backhaus A, Wassenberg F, Sehner S, et al. Improved image quality and low radiation dose with hybrid iterative reconstruction with 80 kV CT pulmonary angiography. Eur J Radiol. 2014;83:1962–9. https://doi.org/10.1016/j.ejrad.2014.06.016.
23. Patel R, Blake GM, Fogelman I. Radiation dose to the patient and operator from a peripheral dual X-ray absorptiometry system. J Clin Densitom. 1999;2:397–401. https://doi.org/10.1016/S1094-6950(06)60405-8.
24. Schoepf UJ, Costello P. CT angiography for diagnosis of pulmonary embolism: state of the art. Radiology. 2004;230:329–37. https://doi.org/10.1148/radiol.2302021489.
25. Cao JX, Wang YM, Lu JG, Zhang Y, Wang P, Yang C. Radiation and contrast agent doses reductions by using 80-kV tube voltage in coronary computed tomographic angiography: a comparative study. Eur J Radiol. 2014;83:309–14. https://doi.org/10.1016/j.ejrad.2013.06.032.
26. Sabarudin A, Mustafa Z, Nassir KM, Hamid HA, Sun Z. Radiation dose reduction in thoracic and abdomen–pelvic CT using tube current modulation: a phantom study. J Appl Clin Med Phys. 2015;16:319–28.